

Optical investigations of InN nanodots capped by GaN at different temperatures

C. S. Ku, W. C. Chou, and M. C. Lee

Citation: [Applied Physics Letters](#) **90**, 132116 (2007); doi: 10.1063/1.2716347

View online: <http://dx.doi.org/10.1063/1.2716347>

View Table of Contents: <http://scitation.aip.org/content/aip/journal/apl/90/13?ver=pdfcov>

Published by the [AIP Publishing](#)

Articles you may be interested in

[Selective area growth and characterization of InGaN nano-disks implemented in GaN nanocolumns with different top morphologies](#)

Appl. Phys. Lett. **100**, 231906 (2012); 10.1063/1.4728115

[InN nanocolumns grown by plasma-assisted molecular beam epitaxy on A -plane GaN templates](#)

Appl. Phys. Lett. **94**, 221908 (2009); 10.1063/1.3151824

[Inhomogeneous InGaN and InN with Inenriched Nanostructures](#)

AIP Conf. Proc. **893**, 269 (2007); 10.1063/1.2729871

[High-density InGaN nanodots grown on pretreated GaN surfaces](#)

Appl. Phys. Lett. **89**, 023114 (2006); 10.1063/1.2218312

[InGaN nanorings and nanodots by selective area epitaxy](#)

Appl. Phys. Lett. **87**, 143111 (2005); 10.1063/1.2056584

The advertisement features a dark blue background with white and orange text. At the top left, it reads 'NEW! Asylum Research MFP-3D Infinity™ AFM' in large white letters, followed by 'Unmatched Performance, Versatility and Support' in orange. On the right, the Oxford Instruments logo is shown with the tagline 'The Business of Science®'. Below the text are several images: a textured surface, a circular pattern, a grid of small squares, and the physical AFM instrument. Text boxes describe the instrument's capabilities: 'Stunning high performance', 'Simpler than ever to GetStarted™', 'Comprehensive tools for nanomechanics', and 'Widest range of accessories for materials science and bioscience'.

Optical investigations of InN nanodots capped by GaN at different temperatures

C. S. Ku,^{a)} W. C. Chou, and M. C. Lee

Department of Electrophysics, National Chiao Tung University, Hsinchu 300, Taiwan, Republic of China

(Received 18 January 2007; accepted 20 February 2007; published online 29 March 2007)

InN nanodots capped with GaN for temperatures from 600 to 730 °C were investigated. While the dot emission intensity at 0.77 eV decreased with increasing capping temperature, two extra visible emission bands appeared around 2.37 eV (green band) and 2.96 eV (violet band). Furthermore, x ray diffraction shows that the 71.7° and 70.2° peaks were tentatively attributed to InGaN alloy with In fractions of 14.8% and 34.2%, respectively. Moreover, the near-field measurements helped reveal the regions of different emissions. The violet-band mapping showed a spatial distribution in contrast to nanodot distribution but the green band showed a uniform distribution that apparently reflects the capping induced InGaN alloy. © 2007 American Institute of Physics. [DOI: 10.1063/1.2716347]

InN, the least studied group-III nitride, has attracted intense interests because of its distinctive optical properties.^{1–3} Early reports using infrared absorption technology have shown that the band gap energy of InN is 1.8–2.0 eV.⁴ Recently, numerous studies have observed instead a strong photoluminescence (PL) emission at around 0.7–0.8 eV but explained in different ways such as “free-to-bound” or In clusters related scattering or oxygen related defects, deep level traps, etc.^{5–14} Thus, the luminescence mechanism of InN is still discordant. Furthermore, some reports indicated that the InN nanodots can be grown on GaN using metal organic vapor phase epitaxy (MOVPE). The InN nanodots after proper capping with GaN or AlN layer may be very promising for practical applications. However, systematic studies of the emission properties of embedded InN nanodots in GaN or AlN are still needed, only one encapsulated by SiO₂ being reported.¹⁵ In this letter, we present the optical properties of embedded InN dots on GaN buffer and capped by GaN at different temperatures.

The InN dot samples were grown by MOVPE using trimethyl gallium, trimethyl indium (TMIn), and NH₃ as source materials on GaN/sapphire(0001) at 700 °C. The gas flow sequence basically consists of four steps: 20 s TMIn source step, 20 s NH₃ source step, and the intervened 10 s purge steps during which a small amount of NH₃ ($4.46 \times 10^5 \mu\text{m}/\text{min}$) is introduced intentionally in order to suppress the reevaporation of adsorbed nitrogen atoms. After the growth of InN dots, a continuous flush of NH₃ was provided for the growth of a 35-nm-thick GaN capping layer at the temperature range from 600 to 730 °C. For PL and near-field scanning optical microscopy (NSOM) measurements were performed using the 325 nm He–Cd laser (IK5552R-F) as an excitation source and detected by photomultiplier tube and LN-cooled extended InGaAs photodiode for visible and IR spectral ranges. For the detailed setup, please refer to our early report.¹⁶

We show atomic force microscopy (AFM) images ($2 \times 2 \mu\text{m}^2$) of InN nanodots with/without GaN capping in Fig. 1(a)–1(f). One can see clear hexagonal InN nanodots whose density is $3.9 \times 10^8 \text{ cm}^{-2}$ and the average dot height is 24.3 nm for the uncapped sample; elsewhere the surface

morphology is rather flat. As the capping temperature increased from 600 to 730 °C, the morphology became rough and dots appeared irregularly deformed with dot density and height decreased by less than a factor of 2, and some dots were even merged. These are likely due to the enhanced diffusion of highly mobile indium atoms and indium desorption becoming severe at high capping temperature on the one hand. On the other hand, since the GaN capping layer was deposited at much lower temperatures (in the so-called kinetic mode) than the most suitable growth temperature of 1050 °C, it may cause surface roughness because nitrogen supply is not sufficient. Table I summarizes the average dot density and height taken from larger AFM images.

As shown in Fig. 2, besides the near band edge emission of GaN buffer layer (3.48 eV),¹⁷ we observed clearly the infrared emission at about 0.77 eV for uncapped and capped samples up to 700 °C that is associated with InN band to band transitions. By increasing the capping temperature to 730 °C, this infrared peak intensity decreased drastically. Furthermore, the InN band to band emission peak was from 0.77 to 0.74 eV with increasing the capping temperature. This may due to InGaN formation that reduces confinement barrier and/or small strain effect between InGaN/InN and GaN/InN interfaces. We will discuss below evidences of InGaN formation. However, when the capping temperature was 675 °C, the strong violet emission appeared at 2.96 eV and

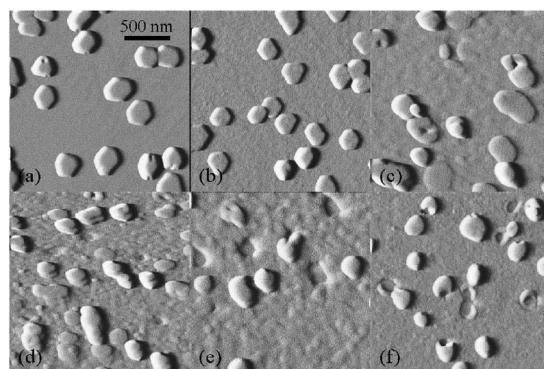


FIG. 1. AFM images ($2 \times 2 \mu\text{m}^2$) of InN nanodots (a) without capping and with different capping temperatures: (b) 600 °C, (c) 675 °C, (d) 700 °C, (e) 715 °C, and (f) 730 °C.

^{a)}Electronic mail: csku.ep88g@nctu.edu.tw

TABLE I. Average dot density and dot height of InN nanodots taken from a $10 \times 10 \mu\text{m}^2$ area.

Sample	a	b	c	d	e	f
Capping temperature	Uncapped	600 °C	675 °C	700 °C	715 °C	730 °C
Dot density (cm^{-2})	3.9×10^8	3.8×10^8	3.5×10^8	3.6×10^8	2.4×10^8	2.5×10^8
Dot height (nm)	24.3	19.8	18.3	15.1	13.5	13.7

its intensity was the strongest at 700 °C. By further raising the temperature, another green emission appeared around 2.37 eV. While the green emission increases, the violet emission decreases as shown in Fig. 2. Obviously, two PL signals are from competitive radiative transitions. Thus, high temperature capping not only degrades and even destroys the infrared emission from InN but also opens up other emission channels. These results conform to the AFM images of deformed nanodots and roughened surface at 715 and 730 °C.

The visible emissions were not expected at first. Their appearance could be from deep levels related to various defects in GaN (Refs. 18–20) and/or due to InGa_N formation at suitable capping temperatures.²¹ To figure out their origins, we used x-ray diffraction (XRD) to analyze the sample composition and NSOM mapping to determine their spatial distribution.

The XRD results show when temperature increased, a broad feature appeared at about 33° that is likely from InN (10 $\bar{1}$ 1),²² In droplet, or some compositional InGa_N. In order to analyze this feature closely, we carried out large angle diffraction and hoped that the large separation between InN and GaN (0004) may reveal more details. Indeed, new features appeared around 70° in Fig. 3(a) that should be associated with the small angle diffraction feature around 33°. After subtracting the strong GaN (0004) signals and proper fitting, we can clearly identify three peaks as shown in Fig. 3(b). For 700 °C capping temperature and above, the appearance of the 69.4° peak is likely associated with the InN (20 $\bar{2}$ 2) peak reported in Refs. 23 and 24. The faceted nanodots that we observed in AFM images may contain both (10 $\bar{1}$ 1) and (20 $\bar{2}$ 2) planes.

Concerning the other two peaks, their appearances are closely related to the PL spectra discussed above. Since no characteristic XRD peak appears for the point defects or native defects of GaN, we tend to believe that the two extra peaks at 70.2° and 71.7° are due to the In_xGa_{1-x}N formation.

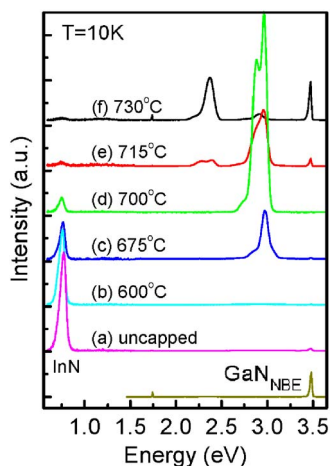


FIG. 2. Capping temperature dependence micro-PL spectra of InN nanodots.

By linear interpolation, the corresponding In content x would be 34.24% and 14.79%.

The band gap energies of these two compositions are calculated to be 2.96 and 2.37 eV, respectively, by adopting the following Vegard law with the bowing parameter $b=0.9$:

$$E_g = xE_{g(\text{InN})} + (1-x)E_{g(\text{GaN})} - bx(1-x). \quad (1)$$

These two energies agree well with the two visible emission bands, violet and green. As shown in Fig. 4, the violet emission (2.96 eV) versus the capping temperature peaked at 700 °C, while the green emission (2.37 eV) becomes increasingly important at 715 and 730 °C and the InN band to band transition is dominant only at 600 and 675 °C. As for the 71.7° and 2.96 eV peaks, they showed a somewhat similar though more complex behavior with the largest intensities between 675 and 700 °C. Moreover, the 65.13° and 70.2° peaks showed the same trend as the PL peaks at 0.77 and 2.37 eV, respectively. Since the PL intensity variation involves a complicated band structure, we can only say that their rising and falling are affected by several competitive radiative transitions. The proper capping temperature may favor certain InGa_N compositions.

With the help of NSOM mapping, we can obtain the spatial distribution of these visible emission signals at room temperature. The 2.88 eV (430 nm) and 2.34 eV (530 nm) were probed due to redshift from 10 K to room temperature. By mapping the surface morphology and taking NSOM images simultaneously, one would be able to decide where the violet and green emission signals are originated.

Figure 5(a)–5(d) showed the NSOM results of the 730 °C capped sample. Image (a) is the mapping of the 364 nm GaN peak. We noticed that PL signals are strong only in the V-defect region and relatively weak elsewhere. The V-defect depth (~100 nm) was deeper than both InN nanodots and the capping layer. There is likely an interface

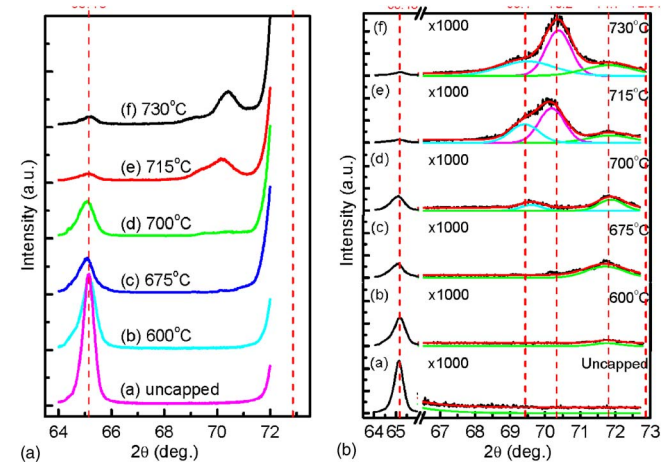


FIG. 3. (a) High angle x-ray diffraction curves of 700 °C grown InN nanodots on GaN films. (b) After subtracting GaN background and the fitting curves.

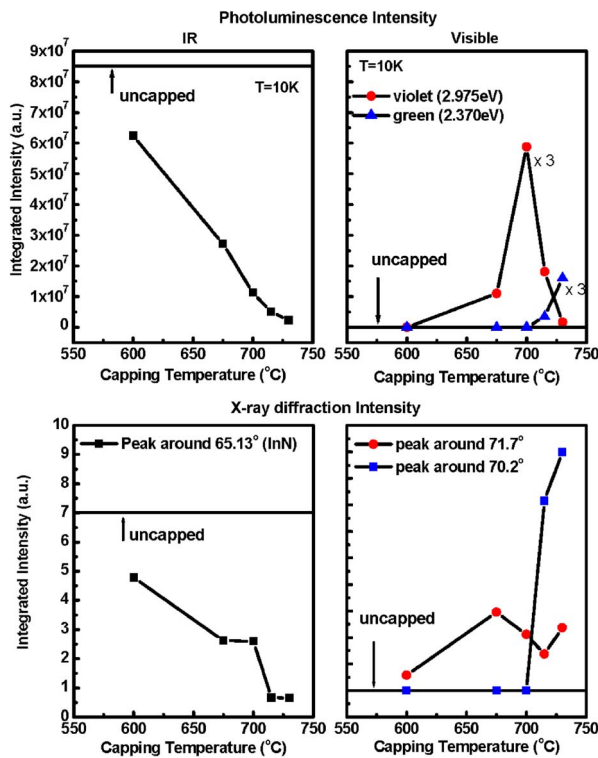


FIG. 4. Integrated intensity of the (a) InN IR peak and (b) violet (2.96 eV) and green (2.37 eV) emission bands.

layer between the GaN buffer layer and InN dot region that may include some compositional InGaN with lower band gap energy. In the PL processes, the 364 nm emission is likely reabsorbed by this interface. Thus, the 364 nm emission occurred only in *V*-defect regions belonging to the GaN buffer layer.

For the violet (430 nm) emission, it is from neither the *V*-defect nor the InN nanodot region [see images (b) and (c)]. We believe that this emission comes from the interface layer (may contain InGaN) formed by capping, because on the one hand, this layer is interrupted in the *V* defect, and on the other hand, the violet emission can also be reabsorbed by InN nanodots with low band gap energy (0.77 eV).

However, the green (530 nm) emission seems to occur over the whole region as shown in Fig. 5(d) with no obvious correlation between the topography and PL signals. We think that the green emission is from the capping layer that might also include compositional InGaN randomly. Since there is no other absorption material on top of this layer, the green emission did cover the whole sample surface. Finally, the capping effect changed the sample properties by showing visible emissions. Their appearance concurred with XRD features that revealed evidence of InGaN alloy formation. The NSOM mapping provides further evidence where they are emitted.

In summary, capping effect on InN dots influences the dot quality and optical properties. We clearly observed that the InN band to band emission appeared at 0.77 eV. Moreover, two extra visible emission bands were observed by increasing the capping temperature and XRD results indicated that are likely due to InGaN formation, although induced defect levels in GaN cannot be excluded. The NSOM mapping revealed the origins of visible PL emission bands that are from the capping layer and the interface layer between

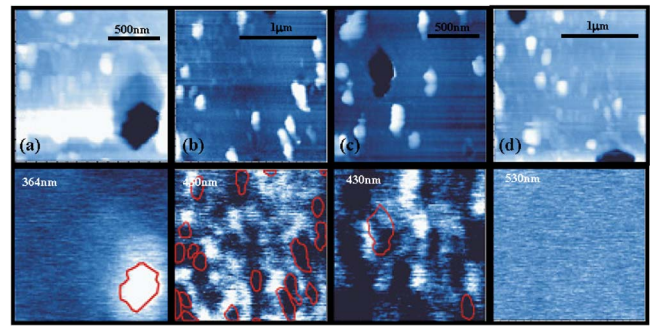


FIG. 5. NSOM topographies and mapping images taken at 300 K of the 730 °C capped sample at (a) 364 nm (*V* defect marked), (b) 430 nm (with nanodots marked), (c) 430 nm (with *V*-defect marked line), and (d) 530 nm.

InN nanodots and GaN layer. The interface layer may contain some InGaN alloy formed by capping processes.

This work has been supported by the National Science Council of the Republic of China under Contract No. NSC94-2120-M-009-016.

- ¹E. Bellotti, B. K. Doshi, K. F. Brennan, J. D. Albrecht, and P. P. Ruden, *J. Appl. Phys.* **85**, 916 (1999).
- ²B. E. Foutz, S. K. O'Leary, M. S. Shur, and L. F. Eastman, *J. Appl. Phys.* **85**, 7727 (1999).
- ³S. K. O'Leary, B. E. Foutz, M. S. Shur, U. V. Bhapkar, and L. F. Eastman, *J. Appl. Phys.* **83**, 826 (1997).
- ⁴T. L. Tansley and C. P. Foley, *J. Appl. Phys.* **59**, 3241 (1986).
- ⁵V. Yu. Davydov, A. A. Klochikhin, R. P. Seisyan, V. V. Emtsev, S. V. Ivanov, F. Bechstedt, J. Furthmuller, H. Harima, A. V. Mudryi, J. Aderhold, O. Semchinova, and J. Graul, *Phys. Status Solidi B* **229**, R1 (2002).
- ⁶J. Wu, W. Walukiewicz, K. M. Yu, J. W. Ager III, E. E. Haller, H. Lu, W. J. Schaff, Y. Saito, and Y. Nanishi, *Appl. Phys. Lett.* **80**, 3967 (2002).
- ⁷T. Matsuoka, H. Okamoto, M. Nakao, H. Harima, and E. Kurimoto, *Appl. Phys. Lett.* **81**, 1246 (2002).
- ⁸B. Arnaudov, T. Paskova, P. P. Paskov, B. Magnusson, E. Valcheva, B. Monemar, H. Lu, W. J. Schaff, H. Amano, and I. Akasaki, *Phys. Rev. B* **69**, 115216 (2004).
- ⁹T. V. Shubina, S. V. Ivanov, V. N. Jmerik, D. D. Solnyshkov, V. A. Vekshin, P. S. Kop'ev, A. Vasson, J. Leymarie, A. Kavokin, H. Amano, K. Shimono, A. Kasic, and B. Monemar, *Phys. Rev. Lett.* **92**, 117407 (2004).
- ¹⁰Q. X. Guo, T. Tankaka, M. Nishio, H. Ogawa, X. D. Pu, and W. Z. Shen, *Appl. Phys. Lett.* **86**, 231913 (2005).
- ¹¹K. S. A. Butcher, *J. Cryst. Growth* **7**, 269 (2004).
- ¹²K. S. A. Butcher, *InN, a Historic review—From obscurity to controversy, Advanced Materials in Electronics*, edited by Qixin Guo (Research Signpost, Kerala, India, 2004), pp. 1–24.
- ¹³D. Alexandrov, K. S. A. Butcher, and M. Wintrebert-Fouquet, *J. Cryst. Growth* **269**, 77 (2004).
- ¹⁴R. Intartaglia, B. Maleyre, S. Ruffenach, O. Briot, T. Taliercio, and B. Gil, *Appl. Phys. Lett.* **86**, 142104 (2005).
- ¹⁵S. Ruffenach, B. Maleyre, O. Briot, and B. Gil, *Phys. Status Solidi C* **2**, 826 (2005).
- ¹⁶C. S. Ku, J. M. Peng, W. C. Ke, H. Y. Huang, N. E. Tang, W. K. Chen, W. H. Chen, and M. C. Lee, *Appl. Phys. Lett.* **85**, 2818 (2004).
- ¹⁷K. Kornitzer, T. Ebner, K. Thonke, R. Sauer, C. Kirchner, V. Schwegler, M. Kamp, M. Leszczynski, I. Grzegory, and S. Porowski, *Phys. Rev. B* **60**, 1471 (1999).
- ¹⁸Sukit Limpijumngong and Chris G. Van de Walle, *Phys. Rev. B* **69**, 035207 (2004).
- ¹⁹Michael A. Reshchikov and Hadis Morkoc, *J. Appl. Phys.* **97**, 061301 (2005).
- ²⁰Jorg Neugebauer and Chris G. Van de Walle, *Appl. Phys. Lett.* **69**, 503 (1996).
- ²¹N. A. El-Masry, E. L. Piner, S. X. Liu, and S. M. Bedair, *Appl. Phys. Lett.* **72**, 40 (1998).
- ²²A. F. Wright and J. S. Nelson, *Phys. Rev. B* **51**, 7866 (1995).
- ²³Hiroyuki Shinoka and Nobuki Mutsukura, *Thin Solid Films* **503**, 8 (2006).
- ²⁴M. F. Wu, S. Q. Zhou, A. Vantomme, Y. Huang, H. Wang, and H. Yang, *J. Vac. Sci. Technol. A* **24**, 2 (2006).